MOVING FINITE ELEMENTS AND APPLICATIONS TO SOME PROBLEMS IN OIL RESERVOIR MODELLING

A. WATHEN

NUMERICAL ANALYSIS REPORT 4/82

MOVING FINITE ELEMENTS AND APPLICATIONS TO SOME PROBLEMS IN OIL RESERVOIR MODELLING

A. Wathen

1. Introduction

Only fairly recently have the problems of injectant driven oil recovery attracted intense mathematical interest. For some references see, for example, [1], [2], [3] and [4].

In this report we look at a mathematical model of the process and consider approximate solutions obtained by a finite element method with moving nodes. We begin by deriving some of the important equations governing the multiphase flow of immiscible fluids in oil reservoirs from the physical conservation laws. We then present the Moving Finite Element Method and introduce some new ideas which we have incorporated into the method. Applications of our method to some simple one-dimensional oil recovery problems are then presented, together with initial conclusions and speculations.

2.1 The Physical Problem

We are principally concerned with the modelling of secondary recovery of hydrocarbon from an underground reservoir. Primary recovery consists of simply allowing the oil to gush out under the pressure of the surrounding strata. Secondary recovery involves injecting some fluid (typically water) into the reservoir at certain wells in order to drive the oil towards other production wells. It is known that sharp fronts form between the injectant and hydrocarbons in many such reservoir floods [5], [6] and it is the modelling of these fronts which is one of our major concerns.

2.2 The Mathematical Problem

Consider the flow of n immiscible phases in an arbitrary region R with boundary ∂R within a reservoir. Conservation of mass of phase π implies the equation

$$\frac{\partial}{\partial t}\int_R \phi\,\rho_\pi S_\pi\,d\tau = -\int_{\partial R} \rho_\pi \underline{u}_\pi \cdot \underline{ds} + \int_R q_\pi\,d\tau \qquad (1)$$

where ϕ is porosity, ρ_π is density, S_π is saturation (fraction of total pore space), $\underline{u}_\pi$ is the flow (Darcy velocity), and q_π is the mass rate injection per unit volume. ($\underline{ds}$ is taken in the direction of the outward normal to R.)

From the Divergence Theorem

$$\int_{\partial R} \rho_\pi \underline{u}_\pi \cdot \underline{ds} = \int_R \nabla\cdot(\rho_\pi \underline{u}_\pi)\,d\tau,$$

so that (1) becomes

$$\int_R \left[\frac{\partial}{\partial t}(\phi\rho_\pi S_\pi) + \nabla\cdot(\rho_\pi \underline{u}_\pi) - q_\pi\right] d\tau = 0.$$

In all the problems that we shall deal with here the wells (sources and sinks) lie on the boundary and will be taken into account by the boundary conditions, so we can put $q_\pi = 0$. Also we shall take the porosity as invariant with time. Then, since R is arbitrary, we have

$$\phi \frac{\partial}{\partial t} (\rho_\pi S_\pi) + \nabla \cdot (\rho_\pi \underline{u}_\pi) = 0. \tag{2}$$

We now relate the flow to the pressure gradient using Darcy's Law, namely,

$$\underline{u}_\pi = \frac{-K\, k_{r\pi}}{\mu_\pi} (\nabla p_\pi - \rho_\pi g \nabla d), \tag{3}$$

where p_π is the pressure, g is gravity, d is depth, K is the absolute permeability of the medium, $k_{r\pi}$ is the relative permeability of the medium to phase π in the presence of other phases, i.e. $k_{r\pi} = k_{r\pi}(S_1, S_2, \ldots, S_n)$ in general, and μ_π is the viscosity.

We expand the derivatives in (2) and divide through by ρ_π to obtain

$$\phi S_\pi c_\pi \frac{\partial p_\pi}{\partial t} + \phi \frac{\partial S_\pi}{\partial t} + \frac{1}{\rho_\pi} \underline{u}_\pi \cdot \nabla \rho_\pi + \nabla \cdot \underline{u}_\pi = 0, \tag{4}$$

where $c_\pi = \frac{1}{\rho_\pi} \frac{d\rho_\pi}{dp_\pi}$ is the phase compressibility.

We then use empirical relations for the capillary pressures, which in their most general form are

$$p_i - p_j = p_{ij}(S_1, S_2, \ldots, S_n) \qquad i \neq j; \text{ (note } p_{kk} = 0).$$

If we now define the average pressure $P = \frac{1}{n} \sum_{j=1}^{n} p_j$

then
$$p_\pi = P + \frac{1}{n} \sum_{j=1}^{n} p_{\pi j} \tag{5}$$

so that (4) becomes

$$\phi S_\pi c_\pi \frac{\partial P}{\partial t} + \phi S_\pi c_\pi \frac{1}{n} \frac{\partial}{\partial t} \left(\sum_{j=1}^{n} p_{\pi j}\right) + \phi \frac{\partial S_\pi}{\partial t} + \frac{1}{\rho_\pi} \underline{u}_\pi \cdot \nabla \rho_\pi + \nabla \cdot \underline{u}_\pi = 0. \tag{6}$$

Now sum equations (6) over all phases π to give

$$\phi \frac{\partial P}{\partial t} \sum_{\pi=1}^{n} S_\pi c_\pi + \frac{\phi}{n} \sum_{\pi=1}^{n} S_\pi c_\pi \frac{\partial}{\partial t} \left(\sum_{j=1}^{n} p_{\pi j}\right) + \sum_{\pi=1}^{n} \frac{1}{\rho_\pi} \underline{u}_\pi \cdot \nabla \rho_\pi + \nabla \cdot \underline{u}_\tau = 0, \tag{7}$$

where we have used the fact that the total pore space is full, namely,

$$\sum_{\pi=1}^{n} S_\pi = 1, \tag{8}$$

and have written $\underline{u}_\tau$ for the total flow $\sum_{\pi=1}^{n} \underline{u}_\pi$.

In general we then have to solve (7) along with $n-1$ of the equations (2) or (4) for the pressure and $n-1$ of the saturations, the final saturation being obtained from (8).

If we assume incompressibility of all phases then (7) simplifies to the form

$$\nabla \cdot \underline{u}_\tau = 0 \tag{9}$$

and (2) becomes

$$\phi \frac{\partial S_\pi}{\partial t} + \nabla \cdot \underline{u}_\pi = 0 \quad . \tag{10}$$

For a horizontal reservoir with permeabilities independent of the vertical direction we may substitute for u_π from (3) in to (10) obtaining

$$\phi \frac{\partial S_\pi}{\partial t} + \nabla \cdot (-\lambda_\pi \nabla p_\pi) = 0, \tag{11}$$

where we have written λ_π for the mobility $Kk_{r\pi}/\mu_\pi$.

If the sources and sinks are also uniform in the vertical direction, then we may integrate vertically to obtain a purely two-dimensional problem. In that case we can treat (3) as

$$\begin{aligned} \underline{u}_i &= -\lambda_i \nabla p_i \qquad (i = 1,\ldots,n) \\ &= -\lambda_i \nabla P - \frac{1}{n} \lambda_i \nabla \Big(\sum_{k=1}^{n} P_{ik}\Big), \end{aligned}$$

from (5). Similarly summing (3) over each phase gives

$$\underline{u}_\tau = -\sum_{j=1}^{n} \lambda_j \nabla p_j = -\sum_{j=1}^{n} \lambda_j \nabla P - \frac{1}{n} \sum_{j=1}^{n} \lambda_j \nabla \Big(\sum_{k=1}^{n} P_{jk}\Big).$$

Thus eliminating ∇P we have

$$\underline{u}_i = \frac{\lambda_i}{\sum_{j=1}^{n} \lambda_j} \underline{u}_\tau + \frac{\lambda_i \frac{1}{n} \sum_{j=1}^{n} \lambda_j \nabla \Big(\sum_{k=1}^{n} P_{jk} - P_{ik}\Big)}{\sum_{j=1}^{n} \lambda_j} \quad . \tag{12}$$

We note in passing that the capillary pressure terms of this expression are of the form

$$\begin{aligned} & f(S_1,\ldots,S_n) \nabla p_{\ell m}(S_1,\ldots,S_n) \\ &= f(S_1,\ldots,S_n) \sum_{i=1}^{n} \frac{\partial p_{\ell m}}{\partial S_i} \nabla S_i, \end{aligned}$$

and that when (12) is used in (10) only the divergence of such terms appear; thus capillary pressure acts as a non-linear diffusion in such problems.

We shall here be interested in modelling the pure convection aspect of such problems and the consequent discontinuous solutions. We thus take the above equations in the limit of zero capillary pressure. Substituting (12) in (10) and using (9), we obtain

$$\phi \frac{\partial S_\pi}{\partial t} + \underline{u}_\tau \cdot \nabla \left(\frac{\lambda_\pi}{\sum_{j=1}^{n} \lambda_j} \right) = 0 \qquad (13)$$

for $\pi = 1,\ldots,n$, together with (9) and (8) to solve for the unknowns S_π ($\pi = 1, \ldots n$) and the common pressure P.

In the simplest case of one-dimensional flow (9) becomes $\frac{\partial}{\partial x} u_\tau = 0$ which gives $u_\tau = h(t)$, i.e. u_τ is purely time dependent.

Hence for a positive total flow (13) becomes

$$\frac{\phi}{h(t)} \frac{\partial S_\pi}{\partial t} + \frac{\partial}{\partial x} \left(\frac{\lambda_\pi}{\sum_{j=1}^{n} \lambda_j} \right) = 0 \qquad (14)$$

Now let $T = \frac{1}{\phi} \int^t h(r)dr$ and write

$$\frac{\lambda_\pi(S_1,\ldots,S_n)}{\sum_{j=1}^{n} \lambda_j(S_1,\ldots,S_n)} = f_\pi(S_1,\ldots,S_n) .$$

Then (14) becomes

$$\frac{\partial S_\pi}{\partial T} + \frac{\partial}{\partial x} f_\pi(S_1,\ldots,S_n) = 0 \qquad (15)$$

In the particular case of two-phase flow we need only seek a solution to one of the equations (15).

So taking $S = S_1$, (so that $S_2 = 1 - S$) and $f_1(S, 1 - S) = f(S)$, we obtain the well-known Buckley-Leverett Equation [7], namely,

$$\frac{\partial S}{\partial T} + \frac{\partial}{\partial x} f(S) = 0 \qquad (16)$$

If we assume that there is no change in reservoir structure (i.e. K = constant) nor in fluid viscosity, then f has the form

$$f(s) = \frac{k_{r1}(S)}{k_{r1}(S) + \frac{\mu_1}{\mu_2} k_{r2}(S)} \quad . \tag{18}$$

The relative permeabilities are determined empirically [5] and it is found that $k_{r\pi}$ is an increasing function of S_π in such a way that f is in general an S-shaped curve as shown in Figure 2.1.

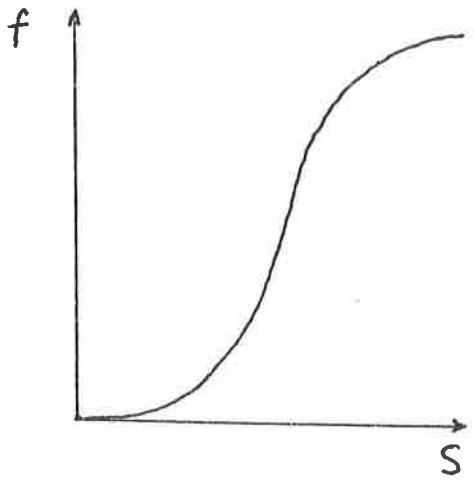

Figure 2.1

2.3 Numerical Methods

We would like to require of any numerical method that it accurately modelled any sharp front moving through a reservoir. In particular for the problem of 2-phase immiscible incompressible flow in the zero capillary pressure limit described above, a major consideration for any numerical scheme is that it should reproduce the strength and speed of the shock accurately. We are particularly interested in the amount of hydrocarbon displaced before 'breakthrough', i.e. the instant when the bank of injected fluid behind the shock reaches the production well [5]. If this can be accurately estimated for different injection strategies then the reservoir engineer is in a position to more confidently choose an optimal strategy.

Most numerical reservoir simulators use standard finite difference methods on fixed rectangular grids (see for example [8], [9]).
Though this facilitates the inclusion of many complicated features and the use of the most general equations describing the flows, the modelling of sharp fronts is a major difficulty except on very fine grids.

Also the non-convexity of the fractional flow function f in the Buckley-Leverett equation (16) can cause problems for standard methods [10], this equation lying outside the well studied class of hyperbolic conservation laws with convex fluxes (see e.g. [11], [12]).

In [1] Concus & Proskurowski solve the Riemann problem for the S-shaped flux and present a successful solution of immiscible 2-phase flow equations using the Random Choice Method of Glimm and Chorin.

In this report we describe a new approach based on Moving Finite Elements which is a modification of the work of Keith Miller [13,14], and show the results of applying it to some simple one-dimensional test problems, in particular to the Buckley-Leverett equation.

In section 3.1 we outline the basic method and describe briefly the methods of Miller and of Herbst et al.[15]. In Section 3.2 we analyse the basic method in some detail and prove some results concerning various important features of the method. In 3.3 we deal with the fundamental problem of parallelism in the MFE method. In 3.4 we present our algorithm for the treatment of shocks.

In section 4 we show solutions that have been obtained to a number of problems - principally those of section 2. Finally, in section 5 we state some conclusions based on our initial experience with moving finite elements and their application, and plans for further work.

3.1 The Moving Finite Element Method

Using essentially the notation of [16] we seek a semi-discrete approximate solution of the form

$$v(x,t) = \sum_{j=1}^{N} a_j(t)\alpha_j(x,\underset{\sim}{s}(t)) \tag{19}$$

to the evolutionary equation

$$u_t - L(u) = 0, \tag{20}$$

where L is a general non-linear spacial differential operator. Here $\underset{\sim}{s} = (s_1, s_2, \ldots, s_N)$ is a vector of (time dependent) nodal positions, α_j is any standard finite element basis function on the grid represented by $\underset{\sim}{s}$ and a_j is the usual finite element time dependent nodal amplitude. For a fixed mesh finite element method the nodal positions would not move, but in the present method we allow each of the s_i to vary with time.

Partial differentiation yields

$$v_t = \sum_{j=1}^{N} \{\dot{a}_j(t)\frac{\partial v}{\partial a_j} + \dot{s}_j(t)\frac{\partial v}{\partial s_j}\}$$

$$= \sum_{j=1}^{N} \{\dot{a}_j(t)\alpha_j(x,\underset{\sim}{s}(t)) + \dot{s}_j\beta_j(x,\underset{\sim}{a}(t), \underset{\sim}{s}(t))\} \tag{21}$$

where $\cdot$ denotes total time differentiation.

The function β_j may be regarded as a second type of basis function. It is in general discontinuous even when the corresponding α_j is continuous, but it has the same support as α_j.

Equations to determine the $2N$ parameters a_i, s_i, $i=1,\ldots,N$ may be derived by minimising the square of the L_2 norm of the residual,

$$\| v_t - L(v) \|_{L_2}^2 \tag{22}$$

with respect to the time derivatives of the parameters a_i, s_i, $i=1,\ldots,N$. That is, setting $R = v_t - L(v)$ we seek

$$\min_{\dot{a}_i,\dot{s}_i,i=1,\ldots N} \| R \|_{L_2}^2 \tag{22a}$$

This gives the set of 2N equations

$$< v_t - L(v), \alpha_i > = 0 = < v_t - L(v), \beta_i > \qquad (23)$$

for $i=1,\ldots,N$.

Here $<,>$ denotes the L_2 inner product. Evaluating the inner products and writing y as a vector of the a_i and s_i $(i=1,\ldots,N)$, in some arrangement, we can express these equations as a non-linear ordinary differential equation system of the form

$$A(y)\,\dot{y} = g(y) \,. \qquad (24)$$

This non-linear system of ordinary differential equations is then solved by some time-stepping scheme.

For the specific case of piecewise linear finite elements in one-dimension, v has the form shown in Fig. 3.1, the basis function α_i being the 'hat' function (shown in Fig. 3.2).

$$\alpha_i = \begin{cases} \dfrac{x - s_{i-1}}{\Delta s_i} & \text{for } s_{i-1} \le x \le s_i \\[2ex] \dfrac{s_{i+1} - x}{\Delta s_{i+1}} & \text{for } s_i \le x \le s_{i+1} \\[2ex] 0 & \text{otherwise} \end{cases} \qquad (25)$$

where $\Delta p_i = p_i - p_{i-1}$.

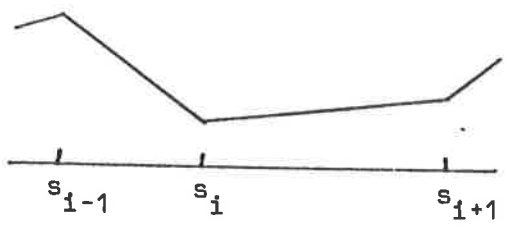

Figure 3.1

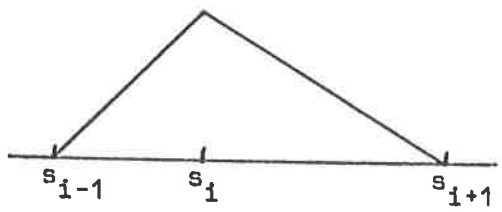

Figure 3.2

The basis function β_i has the form (Figure 3.3)

$$\beta_i = \begin{cases} -m_i\ \alpha_i \text{ for } s_{i-1} \le x < s_i \\ -m_{i+1}\ \alpha_i \text{ for } s_i < x \le s_{i+1} \\ 0 \quad \text{otherwise} \end{cases} \tag{26}$$

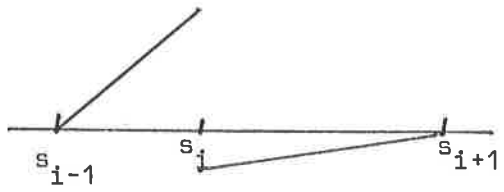

Figure 3.3

where $m_i = \Delta a_i/\Delta s_i$ is the gradient of v on the i^{th} interval.

In the case of a system of equations for $\underline{u} = (u^{(1)},u^{(2)},\ldots,u^{(M)})$,

$$\underline{u}_t^{(k)} - L^{(k)}(\underline{u}) = 0 \qquad (k=1,\ldots,M) \tag{27}$$

we follow Miller in using only one moving grid for all the components, although (as Miller has suggested in [16]) extension could be made to one grid per component, in which case however some interpolation between meshes would be required.

Then, in a similar manner to the above we seek solutions of the form

$$v^{(k)}(x,t) = \sum_{j=1}^{N} v_j^{(k)}(t)\ \alpha_j(x,\underset{\sim}{s}(t)) \qquad (k=1,..,M). \tag{28}$$

Partial differentiation yields

$$v_t^{(k)}(x,t) = \sum_{j=1}^{N} \{\dot{v}_j^{(k)}(t)\ \alpha_j(x,\underset{\sim}{s}(t)) + \dot{s}_j(t)\beta_j^{(k)}(x,\underset{\sim}{v}^{(k)}(t),\underset{\sim}{s}(t))\} \tag{29}$$

where, for piecewise linears, we now have

$$\beta_i^{(k)} = \begin{cases} -m_i^{(k)}\alpha_i & s_{i-1} \le x < s_i \\ -m_{i+1}^{(k)}\alpha_i & s_i < x \le s_{i+1} \\ 0 & \text{otherwise} \end{cases} \tag{30}$$

with $m_i^{(k)} = \Delta v_i^{(k)}/\Delta s_i$ and α_i is the 'hat' function as before for the scalar problem.

We now depart from Miller's approach. Writing $\underline{R} = (R^{(1)},\ldots,R^{(M)})$ as the vector of residuals

$$R^{(k)} = v_t^{(k)} - L^{(k)}(\underline{v}) \tag{31}$$

we propose to minimise

$$\| (\underline{R}^T W \underline{R})^{\frac{1}{2}} \|_{L_2}^2 \tag{32}$$

with respect to each $\dot{v}_i^{(k)}$ $(i=1,\ldots,N)$, $(k=1,\ldots,M)$ and $\dot{s}_i$ $(i=1,\ldots,N)$ where W is some positive definite weighting matrix. For example, for $M = 2$ with $W = \begin{bmatrix} W_1 & W_3 \\ W_3 & W_2 \end{bmatrix}$ this leads to

$$W_1 \langle v_t^{(1)} - L^{(1)}(\underline{v}), \alpha_i \rangle + W_3 \langle v_t^{(2)} - L^{(2)}(\underline{v}), \alpha_i \rangle = 0 \tag{33}$$

$$W_3 \langle v_t^{(1)} - L^{(1)}(\underline{v}), \alpha_i \rangle + W_2 \langle v_t^{(2)} - L^{(2)}(\underline{v}), \alpha_i \rangle = 0 \tag{34}$$

and

$$W_1 \langle v_t^{(1)} - L^{(1)}(\underline{v}), \beta_i^{(1)} \rangle + W_3 \langle v_t^{(1)} - L^{(1)}(\underline{v}), \beta_i^{(2)} \rangle$$

$$+ W_3 \langle v_t^{(2)} - L^{(2)}(\underline{v}), \beta_i^{(1)} \rangle + W_2 \langle v_t^{(2)} - L^{(2)}(\underline{v}), \beta_i^{(2)} \rangle = 0 \tag{35}$$

which we can again write in the form

$$A(y)\dot{y} = g(y) \tag{36}$$

and solve by some time-stepping scheme.

Miller [13,14] chooses to add 'regularisation' terms to the minimisation problems (22) and (32) (where he uses a diagonal weighting matrix W). For the scalar case he solves the following problem:

$$\underset{\dot{a}_i,\dot{s}_i\,(i=1,\ldots,N)}{\text{minimise}} \{ \| v_t - L(v) \|_{L_2}^2 + \sum_{j=2}^{N} (\epsilon_j \Delta\dot{s}_j - S_j) \}. \tag{37}$$

Examples of the regularisation functions ϵ_j and S_j that are used (see [16]) are

$$\epsilon_j = \frac{K_2}{\Delta s_j - K_1} + K_3 , \qquad S_j = \frac{K_4}{\Delta s_j - K_1} \tag{38}$$

where K_i are (small) constants. The S_j functions are termed "inter-nodal

spring functions" and are designed to prevent 'node overtaking'. The ε_j functions are called "inter-nodal viscous forces" and their purpose is to override the problem of parallelism dealt with in section 3.3 of this report.

Herbst, Mitchell and Schoombie [15], concerned about Miller's treatment of inner products of second derivatives with the discontinuous basis functions β_j, have used instead a moving Petrov-Galerkin method. They solved

$$\langle v_t - L(v), \psi_i \rangle = 0 = \langle v_t - L(v), w_i \rangle \quad (i=1,\ldots,N)$$

where v and v_t are as in (19) and (21) and the ψ_i and w_i are Hermite cubic test function on a moving mesh. Further, using a truncation error analysis, they noted that their method gives the exact solution to the equation

$$u_t + f_x(u) = 0$$

for quadratic flux functions f, so long as the classical solution exists. Our analysis in the next section reproduces this result for the standard method, but from a different point of view.

3.2 Analysis of the Method

Following Miller & Miller [13] we may regard the approximate MFE solution v as a point in a non-linear manifold M parameterised by the 2N parameters $\{a_i, s_i, i=1,\ldots,N\}$. Then the time derivative of v

$$v_t = \sum \dot{a}_j \alpha_j + \dot{s}_j \beta_j$$

lies in the tangent space T_v to M at v. T_v is a linear space with basis $\{\alpha_i, \beta_i, i=1,\ldots,N\}$.

Note that, since in (x_{j-1}, x_j), $v_x = -m_j(\alpha_{j-1} + \alpha_j)$ and $vv_x = -m_j(a_{j-1}\alpha_{j-1} + a_j\alpha_j)$ we have

$$v_x = \sum_{j=1}^{N} a_j \alpha_j' = -\sum_{j=1}^{N} \beta_j \tag{39}$$

(where $'$ denotes the spacial derivative), and

$$vv_x = (\tfrac{1}{2}v^2)_x = \sum_{j=1}^{N} a_j \alpha_j \sum_{k=1}^{N} a_k \alpha_k' = -\sum_{j=1}^{N} a_j \beta_j \tag{40}$$

Both lie in the tangent space T_v, and therefore so does $bvv_x + cv_x$, where b, c are constants. An equivalent statement is that, for the initial value

problem

$$u_t + f_x(u) = 0 \tag{41}$$

with

$$f(u) = bu^2 + cu + d \tag{42}$$

and piecewise linear initial data $u(0,x) = u_0(x)$, the standard MFE equations (23) are uniquely satisfied by the exact solution

$$\dot{a}_i = 0, \qquad \dot{s}_i = 2ba_i + c \qquad\qquad i=1,\ldots,N \tag{43}$$

so long as this classical solution exists.

This result does not extend beyond quadratic flux functions f: one can easily show for example that for a cubic flux function

$$v^2 v_x \notin T_v .$$

In fact consideration of higher order piecewise polynomial approximate solutions v to conservation equations of the type (41) is of no help in extending the above result to more general flux functions f because of the following argument.

Let $P_N[x]$ be the piecewise polynomials of degree N in x. Take $u = g(x)$ as initial data for the equation

$$u_t + f_x(u) = 0$$

i.e.

$$u_t + a(u)u_x = 0 \tag{44}$$

where $a(u) = f'(u)$. Then the classical solution after unit time is given by

$$(x,u) \longmapsto (x',u'),$$

where $u' = g(x)$ and $x' = x + a(u)$

$$= x + a(g(x))$$

$$= x + [a\circ g](x)$$

$$= [1 + a\circ g](x) .$$

So if the inverse exists

$$x = [1 + a\circ g]^{-1}(x')$$

which implies that $u' = g([1+a\circ g]^{-1}(x'))$.

Hence $u = g(x) \in P_N[x]$ implies that $u' \in P_N[x']$ $\forall g$

$\Leftrightarrow [1 + a \circ g]^{-1}$ is piecewise linear $\forall g$

$\Leftrightarrow 1 + a \circ g$ is piecewise linear $\forall g$

$\Leftrightarrow a \circ g$ is piecewise linear $\forall g$.

But $g \in P_N[x]$ implies that $a \circ g$ is piecewise linear if and only if $g \in P_1[x]$ and a is linear.

Thus $u \in P_N[x]$ is transformed to $u' \in P_N[x']$ under the equation (44) only when $N = 1$ and for a linear wavespeed $a(u)$.

Now note that the non-linear problem of least squares L_2 - fitting of a function $h(x)$ by some v of the form

$$v = \sum_{j=1}^{N} a_j \alpha_j(x, \underset{\sim}{s}) \in M \tag{45}$$

is to minimise

$$\| h(x) - \sum_{j=1}^{N} a_j \alpha_j(x, \underset{\sim}{s}) \|_{L_2} \quad \text{w.r.t. } a_i, s_i, (i=1,\ldots,N) \tag{46}$$

which leads to the canonical equations

$$\langle h-v, \alpha_i \rangle = 0 = \langle h-v, \beta_i \rangle \qquad (i=1,\ldots,N). \tag{47}$$

Moreover, the problem of L_2-fitting in T_v is to

$$\underset{c_i, d_i, (i=1,\ldots,N)}{\text{minimise}} \| h(x) - \sum_{j=1}^{N} \{c_j \alpha_j + d_j \beta_j\} \|_{L_2} \tag{48}$$

and leads to

$$\langle h - \sum_{j=1}^{N} c_j \alpha_j + d_j \beta_j \, , \alpha_i \rangle = 0 = \langle h - \sum_{j=1}^{N} c_j \alpha_j + d_j \beta_j \, , \beta_i \rangle \quad (i=1,\ldots,N) \tag{49}$$

where α_i and β_i are given by the parameterisation of v.

Thus the MFE equations

$$\langle v_t - L(v) \, , \alpha_i \rangle = 0 = \langle v_t - L(v), \beta_i \rangle \quad (i=1,\ldots,N) \tag{50}$$

give v_t the best L_2 fit in T_v to $L(v)$.

In view of this result and the work of Cullen & Morton [17] and Johnson, Lewis & Morgan [18] on the L_2 fitting properties of fixed finite element methods for hyperbolic problems, we have investigated the hypothesis that the MFE

similarly carries approximately the best L_2 fit to the solution.

In a numerical experiment consisting of initial piecewise linear data (with compact support), we computed the exact solution at some later time t to equation (41) with a non-quadratic flux and then obtained the best L_2 fit to this (classical) solution. We then compared this best fit to the MFE solution at the same time t. We present a sample of the results in Tables 3.1 and 3.2.

A simple 'θ' time-stepping method is used to solve the ordinary differential equation system (24) using Newton iteration to solve the resulting implicit algebraic system. The time truncation error is therefore $O(\Delta t^2)$ for Crank-Nicolson ($\theta = \frac{1}{2}$) and $O(\Delta t)$ for all other θ.

The initial data was chosen purely because the Newton iteration converged fairly rapidly in the L_2 fitting stage with such data. In each pair of columns in Tables 3.1 & 3.2 the first column are the amplitudes and the second the nodal positior that is a_i's and s_i's respectively when considered in the form of (45). The 'exact nodes' column gives the amplitudes (which remain constant) and the positions to which the nodes in the initial data move exactly. The other two columns are self-explanatory, and it can be seen how much closer they are to each other than to the 'exact nodes', particularly for small t when the time discretization effects are smaller.

For the quadratic flux function (42) note that the exact solution (43) of the semi-discrete MFE equations (23) is linear in the dependent variables. Thus any first order approximation to the time derivative will give the exact solution for any Δt so long as the classical solution exists. In particular the simple fully explicit Euler time-stepping (which needs no non-linear solver) produces the exact solution for such problems up to the formation of a shock.

On the basis of this property it was initially thought that any flux function could be approximated by a quadratic spline, and thus we could exactly solve an approximate problem if we put MFE nodes at the knots of the spline. We are still looking into this idea, particularly as a guide to the error analysis. It is

Results for the equation $u_t + u^2 u_x = 0$

Initial data		Exact nodes		L_2 fit to exact solution		MFE with Crank-Nicolson time-stepping		Time
0	0	0	0	3.7E-12	-.0270	-4.2E-10	-.0274	
.9	.2	.9	.362	.9112	.3386	.9136	.3413	
.2	.6	.2	.608	.1921	.5957	.1885	.5959	.2
.7	.7	.7	.798	.6873	.7844	.6881	.7846	
0	1	0	1	5.2E-12	.9830	6.1E-10	.9840	
		0	0	3.5E-8	-.0135	-8.3E-10	-.0136	
		.9	.281	.9059	.2689	.9068	.2698	
		.2	.604	.1959	.5984	.1945	.5984	.1
		.7	.749	.6937	.7428	.6938	.7429	
		0	1	-7.8E-10	.9917	6.0E-10	.9919	
		0	0	1.9E-10	-.002699	4.8E-10	-.002703	
		.9	.2162	.901312	.213788	.901346	.213831	
		.2	.6008	.199000	.599745	.198952	.599744	.02
		.7	.7098	.698725	.708677	.698735	.708685	
		0	1	-5.5E-12	.998365	1.2E-10	.998370	
		0	0	1.0E-11	-.001346	2.4E-10	-.001351	
		.9	.2081	.900654	.206892	.900672	.206908	
		.2	.6004	.199500	.599878	.199479	.599876	.01
		.7	.7049	.699365	.704347	.699366	.704349	
		0	1	-3.4E-13	.999183	6.7E-11	.999185	

TABLE 3.1

Results for the equation $u_t + \frac{\partial}{\partial x} \frac{u^2}{u^2+\frac{1}{2}(1-u)^2} = 0$

Initial data		Exact nodes		L_2 fit to exact solution		MFE with fully explicit Euler time-stepping		Time
0	0	0	0	-2.9E-12	.029539	9.9E-13	.025923	
.9	.2	.9	.202710	.883227	.214567	.884263	.214958	
.2	.6	.2	.624691	.206554	.644133	.205280	.641872	.02
.7	.7	.7	.714674	.719076	.727352	.719830	.727024	
0	1	0	1	1.2E-11	1.017533	-9.5E-12	1.016790	
		0	0	-5.9E-10	.013973	4.1E-13	.013030	
		.9	.201355	.891787	.207223	.892076	.207295	
		.2	.612346	.203072	.621594	.202821	.620843	.01
		.7	.707337	.709638	.713738	.709549	.713822	
		0	1	2.2E-9	1.008491	-6.1E-12	1.008200	

TABLE 3.2

found in practice, however, for a Buckley-Leverett type fractional flow function f (as in Fig. 2.1) that large time steps can be taken with a fully explicit scheme even when shocks are present. This can be explained heuristically by arguing that the nodes approximately follow the characteristics and thus we are not limited to the same extent as with a conventional method (or difference method) - but see recent work of Leveque [20] - in how far we can stably propagate information in a single time step.

In order to move away from the speciality of problems of the type (41), where the characteristics are straight lines, we have considered also the equivalent Buckley-Leverett problem with cylindrical symetry (in which case the characteristics are parabolas) to see whether explicit time discretization was still acceptable. The solutions obtained are shown in Section 4.

3.3 The Problem of Parallelism

It is well known ([13], [15], [16]) that the MFE matrix A of equation (24) becomes singular if and only if the gradients of v on adjacent cells become the same. This fundamental problem we term 'parallelism'.

If $m_j = m_{j+1}$ then we see from (25) and (26) that

$$\beta_j = - m_j \alpha_j \qquad \text{for all } x$$

and thus the two equations $\quad \langle v_t - L(v), \alpha_j \rangle = 0$

$$\text{and} \qquad \langle v_t - L(v), \beta_j \rangle = 0$$

of (23) become linearly dependent; hence A is singular.

Proving the converse is more technical. When we explicitly evaluate the inner products in (23) and order the vector y of (24) as $(a_1, s_1; a_2, s_2; \ldots; a_N, s_N)$ we obtain the $(2i-1)^{th}$ equation of (24) as

$$\frac{1}{6}\Delta s_i \dot{a}_{i-1} - \frac{1}{6}\Delta a_i \dot{s}_{i-1} + \frac{1}{3}(\Delta s_i + \Delta s_{i+1})\dot{a}_i - \frac{1}{3}(\Delta a_i + \Delta a_{i+1})\dot{s}_i + \frac{1}{6}\Delta s_{i+1}\dot{a}_{i+1} - \frac{1}{6}\Delta a_{i+1}\dot{s}_{i+1}$$

$$= \langle L(v), \alpha_i \rangle \qquad (51)$$

and the $2i^{th}$ equation as

$$\frac{1}{6}\Delta a_i \dot{a}_{i-1} + \frac{1}{6}m_i \Delta a_i \dot{s}_{i-1} - \frac{1}{3}(\Delta a_i + \Delta a_{i+1})\dot{a}_i + \frac{1}{3}(m_i \Delta a_i + m_{i+1}\Delta a_{i+1})\dot{s}_i - \frac{1}{6}\Delta a_{i+1}\dot{a}_{i+1} + \frac{1}{6}m_{i+1}\Delta a_{i+1}\dot{s}_{i+1}$$

$$= \langle L(v), \beta_i \rangle \qquad (52)$$

Thus with this ordering of y the matrix A is block 2×2 triple diagonal and is symmetric. So we may write

$$A = \frac{1}{6} \begin{bmatrix} A_1 & B_1 & & & & \\ B_1 & A_2 & B_2 & & & \\ & B_2 & \ddots & \ddots & & \\ & & \ddots & A_i & B_i & \\ & & & B_i & \ddots & \ddots \\ & & & & \ddots & A_N \end{bmatrix} . \tag{53}$$

Then

$$B_{i-1} = \begin{bmatrix} \Delta s_i - \Delta a_i & \\ -\Delta a_i & m_i \Delta a_i \end{bmatrix}, \quad A_i = \begin{bmatrix} 2(\Delta s_i + \Delta s_{i+1}) - 2(\Delta a_i + \Delta a_{i+1}) & \\ -2(\Delta a_i + \Delta a_{i+1}) & 2(m_i \Delta a_i + m_{i+1} \Delta a_{i+1}) \end{bmatrix} \text{ and } B_i = \begin{bmatrix} \Delta s_{i+1} - \Delta a_{i+1} & \\ -\Delta a_{i+1} & m_{i+1} \Delta a_{i+1} \end{bmatrix} . \tag{54}$$

Assume for the present that

$$s_0 < s_1 < \ldots < s_i < \ldots < s_{N+1} \tag{55}$$

so that $\Delta s_i > 0$ for all i. Then we consider the following cases:

Case 1 for $2 \le i \le N-1$, consider the $(2i-1)^{th}$ row. Since the $(1,1)$ element of B_{i-1} and of B_i are strictly positive, the $(2i-1)^{th}$ row of A must be linearly independent of all other rows, except possibly the $2i^{th}$, because of the structure of A. Further, these two rows become linearly dependent only if for some constant p all the following hold:

(a) $p\Delta s_i = \Delta a_i$ (b) $p\Delta a_i = m_i \Delta a_i$

(c) $p(\Delta s_i + \Delta s_{i+1}) = \Delta a_i + \Delta a_{i+1}$ (d) $p(\Delta a_i + \Delta a_{i+1}) = m_i \Delta a_i + m_{i+1} \Delta a_{i+1}$

(e) $p\Delta s_{i+1} = \Delta a_{i+1}$ (f) $p\Delta a_i = m_{i+1} \Delta a_{i+1}$:

(a) => $p = m_i$ and (e) => $p = m_{i+1}$ and it is seen that $p = m_i = m_{i+1}$ satisfies all the other equations (b), (c), (d) and (f).

Case 2 for $2 \le i \le N-1$, consider the $2i^{th}$ row. This is zero if and only if $\Delta a_i = 0 = \Delta a_{i+1}$ that is if and only if $m_i = 0 = m_{i+1}$. So assuming that $\Delta a_i \neq 0$, this row can only depend on rows $2i-2$ and $2i-3$, and this can only happen if $\Delta a_{i+1} = 0$ and (i) $\Delta a_{i-1} = 0$ for $i > 2$ or (ii) for $i = 2$. Consider these situations separately.

(i) this dependence occurs only if there is a constant p such that

(a) $p\Delta a_i = 2\Delta a_i$ (b) $pm_i\Delta a_i = 2m_i\Delta a_i$

(c) $2p\Delta a_i = \Delta a_i$ (d) $2pm_i\Delta a_i = m_i\Delta a_i$

which is clearly not the case.

(ii) this dependence occurs only if there are constants p and q such that

(a) $2p(\Delta s_1+\Delta s_2) - 2q(\Delta a_1+\Delta a_2) = -\Delta a_2$ (b) $-2p(\Delta a_1+\Delta a_2) + 2q(m_1\Delta a_1+m_2\Delta a_2)=m_2\Delta a_2$

(c) $p\Delta s_2 - q\Delta a_2 = -2\Delta a_2$ and (d) $-p\Delta a_2 + qm_2\Delta a_2 = 2m_2\Delta a_2$.

Equation (c) => $p = (q-2)m_2$ which satisfies (d). Substituting this respectively in (a) and (b) gives (e) $-2q(m_1-m_2)\Delta s_1 - 2m_2\Delta s_1 = -\Delta a_2$ and (f) $2q(m_1-m_2)\Delta a_1 + 4m_2\Delta a_1 = m_2\Delta a_2$.

Now if $m_1 = 0$ then (f) => $m_2\Delta a_2 = 0$ which contradicts our initial assumption. So for $m_1 \neq 0$

$m_1 \times$ (e) gives $-2q(m_1-m_2)\Delta a_1 - 4m_2\Delta a_1 = -m_1\Delta a_2$

which when added to (f) implies $m_1 = m_2$ since we have assumed that $\Delta a_2 \neq 0$.

We could have assumed $\Delta a_{i+1} \neq 0$ and similarly derived corresponding results to the above.

The final case we have to consider is

Case 3 rows 1 and 2 (and equivalently rows N and N-1).

These two rows are dependent only if there exists a constant p such that

(a) $p(\Delta s_1+\Delta s_2) = \Delta a_1+\Delta a_2$ (b) $p(\Delta a_1+\Delta a_2) = m_1\Delta a_1 + m_2\Delta a_2$

(c) $p\Delta s_2 = \Delta a_2$ and (d) $p\Delta a_2 = m_2\Delta a_2$.

Equation (c) implies $p = m_2$ which satisfies (d). Substituting this into (a) gives $m_1 = m_2$ which also satisfies (b).

Thus on the assumption (55) we have shown that each row of A is independent of all other rows except when $m_i = m_{i+1}$ for some i. Thus A become singular if and only if we have parallelism.

We shall order the nodes in our method such that (55) always holds, except at a shock where we shall require that just one difference Δs_i be zero - see the next section. We note, however, that with our shock algorithm the matrix A becomes decoupled into two submatrices of the same form, that is that for some i the submatrix B_i is the zero matrix. (We also delete some rows but this does not affect our argument here). Thus the result above applies to each submatrix and hence holds for the whole matrix A even in the presence of shocks.

As we have mentioned before, Miller introduces the regularisation functions ε_j of (38) to 'carry nodes along' when parallelism occurs. In our algorithm we test for parallelism (in fact near-parallelism corresponding to computational singularity) and remove the $(2i-1)^{th}$ equation from the system when $|m_i - m_{i+1}|$ becomes less than some tolerance. However, we must now choose how to update the coefficient a_i. Since we are solving conservation type equations we have in the numerical examples of Section 4 chosen to set $\dot{a}_i = 0$. One could however let the update of a_i be some mean of a_{i-1} and a_{i+1} for example. The important point is that the node s_i is still left free to move, and experiment shows that for any reasonable choice of update for a_i, the node moves to take account of this choice.

If the solution is actually 'flat' at some node ($\Delta a_i = 0 = \Delta a_{i+1}$) one could correspondingly remove the $2i^{th}$ equation (which is $0 = 0$), leaving the $(2i-1)^{th}$ equation to determine the value of a_i at the next time level, and set s_i to be some mean of s_{i-1} and s_{i+1}. For problems of the type (41), however, a node in a flat part of the solution carries no information and simply causes degeneracy of the parameterization. We therefore remove such a node.

There are examples of the effect of this algorithm in Section 4.

3.4 Treatment of Shocks

With no explicit treatment of shocks the standard MFE method results in node-overtaking. Miller's method (see [16]) relies on the introduction of a small viscosity term to prevent this occurring, and on choosing the parameters K in (38) so as to resolve any expected sharp front.

We have applied the Rankine-Hugoniot shock condition directly. With a moving mesh method this is much simpler and more natural to apply than on a fixed mesh.

Our algorithm for equations of the type (41) is:

I. Detect the formation of a shock - that is $s_i \geq s_{i+1}$ for some i.

II. Set $s_i = s_{i+1}$ = some mean of the old position, chosen to approximately ensure conservation.

III. Impose
$$\dot{s}_i = \dot{s}_{i+1} = \frac{f(a_i) - f(a_{i+1})}{a_i - a_{i+1}} \tag{56}$$
to 'shocked' nodes allowing a_i and a_{i+1} to be distinct and to vary in order to represent the strength of the shock.

IV. Delete nodes that become intermediate within the shock front as the solution progresses.

The important step III has the effect of a <u>natural</u> internal boundary condition in that we impose the physical speed of a shock by using the Rankine-Hugoniot conditions, but allow the strength of the shock to be found as part of the solution. As we remarked in Section 3.3., the effect of this procedure is to separate the MFE matrix into two submatrices of the same form, and thus causes no problems of matrix singularity. Note also that a shock is defined by the minimum possible number of nodes (i.e. two) and thus we have no wastage of nodes in modelling a shock.

For our first attempts to treat shocks for systems of equations we have used essentially the same algorithm, but have imposed the speed in III to be a weighted average of the speeds obtained for the separate components, the weighting

being determined by the change in that component. For example, for the system of two equations

$$u_t^{(1)} + f_x^{(1)}(u^{(1)},u^{(2)}) = 0$$

$$u_t^{(2)} + f_x^{(2)}(u^{(1)},u^{(2)}) = 0$$

III becomes $\dot{s}_i = \dot{s}_{i+1} = w \dfrac{f^{(1)}(u_i^{(1)},u_i^{(2)}) - f^{(1)}(u_{i+1}^{(1)},u_{i+1}^{(2)})}{u_i^{(1)} - u_{i+1}^{(1)}}$

$$+ (1-w) \frac{f^{(2)}(u_i^{(1)},u_i^{(2)}) - f^{(2)}(u_{i+1}^{(1)},u_{i+1}^{(2)})}{u_i^{(2)} - u_{i+1}^{(2)}} \qquad (57)$$

where w is chosen depending on the changes in $u_i^{(1)} - u_{i+1}^{(1)}$ and $u_i^{(2)} - u_{i+1}^{(2)}$.

4. Numerical Results

The first two figures of this section are included to display the exact solution properties of the MFE method (43) when used with fully explicit Euler time-stepping. Figure 4.1 represents an initial square wave - the gradients are in fact 10^9. (One would usually expect a graph plotter to plot the line $y = 0$ along the axis!). Figure 4.2 is the MFE solution to the scalar wave equation

$$u_t + u_x = 0$$

with this initial data after a single explicit Euler time step of $\Delta t = 80.0$. It is also the exact solution.

Figure 4.3 shows the formation and propagation of a shock using the algorithm of Section 3.4. Here we are solving the inviscid Burger Equation

$$u_t + uu_x = 0$$

and thus again we have the exact solution properties of Section 3.2 with fully explicit Euler time-stepping. Note in particular how we continue to achieve the exact solution even when the shock has formed.

Figure 4.4 shows our solution to the Buckley-Leverett problem in the form treated by Concus and Proskurowski in [1]. In (18) we take $k_{r1} = S^2$ and $k_{r2} = (1-S)^2$ with the ratio of viscosities $\mu_1/\mu_2 = \frac{1}{2}$. The initial data is $\frac{0.1}{0.1+x}$ with the left hand boundary condition held at $S = 1$ to represent injection of the fluid with saturation S. Figure 4.5 shows the exact solution to this problem.

In Figure 4.6 we show the solution to the same equation, but with more realistic initial data designed to represent the situation after injection at the left hand boundary has just started. For boundary conditions modelling the actual injection see for example [19].

Figure 4.7 represents our MFE solution of the cylindrically symmetric Buckley-Leverett type problem. The derivation is similar to that of equation (15); we include it here for two phases only.

In (9) and (13) assume cylindrical symmetry $S = S(r)$ in some annulus $0 < \varepsilon \le r \le R$. Then (9) becomes

$$\frac{1}{r} \frac{\partial}{\partial r} (r u_\tau) = 0$$

which implies that $r u_\tau = h(t)$ so (13) becomes

$$\frac{\phi}{h(t)} \frac{\partial s}{\partial t} + \frac{1}{r} \frac{\partial}{\partial r} \left(\frac{\lambda_\pi}{\sum_{j=1}^{N} \lambda_j} \right) = 0 .$$

The substitution $T = \frac{1}{\phi} \int^t h(p)dp$

(which now involves a time-stretching with respect to the radial distance r from the well) then gives the equation

$$\frac{\partial S}{\partial T} + \frac{1}{r} \frac{\partial}{\partial r} f(s) = 0$$

which has parabolic characteristics. We emphasise that it is necessary to exclude the origin and thus this equation cannot represent the flow close to the well. However it provides a good test problem.

Our solution to this problem with the initial data of Figure 4.4 shows several of the special features of our method. Note how the shock gradually increases in strength - firstly by moving apart of the two amplitudes of the nodes which initially represent the shock and then, as these nodes are eliminated from the solution, through other nodes which take over the upper and lower amplitudes which define the strength. One can also see the effects of the parallelism algorithm of Section 3.3. The nodes with amplitudes of about 0.7 and about 0.8 are at various time steps throughout this run detected to approximately lie on a straight line. Their amplitudes are then held fixed, and one can see how the nodes adjust.

Finally, Figure 4.8 represents our initial solution of a system of equations of the type (15) which describe the flow of three incompressible immiscible phases with zero capillary pressure. We have taken

$$\lambda_\pi = S_\pi^2 \qquad \text{for} \quad \pi = 1,2,3$$

and put $S_3 = 1-S_1-S_2$ from (8). Thus we have solved the system

$$\frac{\partial S_1}{\partial T} + \frac{\partial}{\partial x}\left(\frac{S_1^2}{S_1^2+S_2^2+(1-S_1-S_2)^2}\right) = 0$$

and

$$\frac{\partial S_2}{\partial T} + \frac{\partial}{\partial x}\left(\frac{S_2^2}{S_1^2+S_2^2+(1-S_1-S_2)^2}\right) = 0 .$$

The saturation S_1 is plotted as the full line and the sum of the saturations $S_1 + S_2$ as the broken line in Fig. 4.8. In this run we have weighted the speed of the first (full line) shock entirely onto the change in S_1 and its corresponding flux, and similarly the second shock is weighted entirely on the change in S_2 and its corresponding flux. We have also in this particular run used a diagonal weighting matrix W so that $W_1 = W_2$ and $W_3 = 0$ in equations (33), (34) and (35).

Conclusions

An accurate and extremely efficient algorithm based on Moving Finite Elements has been developed for the solution of scalar hyperbolic conservation laws in one dimension together with an extension to systems of equations.

Exact solution properties of the semi-discrete method for some simple problems are noted and the hypothesis that these ideas may be extended to more general equations by considering the MFE method to approximately carry the best L_2 fit to the solution is examined. Numerical experimentation tends to confirm this. It is further noted that the fully discrete method with explicit Euler time-stepping has exact solution properties for these simple equations and may be used without any severe stability restriction for more general problems. This gives the method an enormous increase in efficiency over implicit methods. In all of the examples of Section 4 it took considerably longer to plot the graphs than to produce the results.

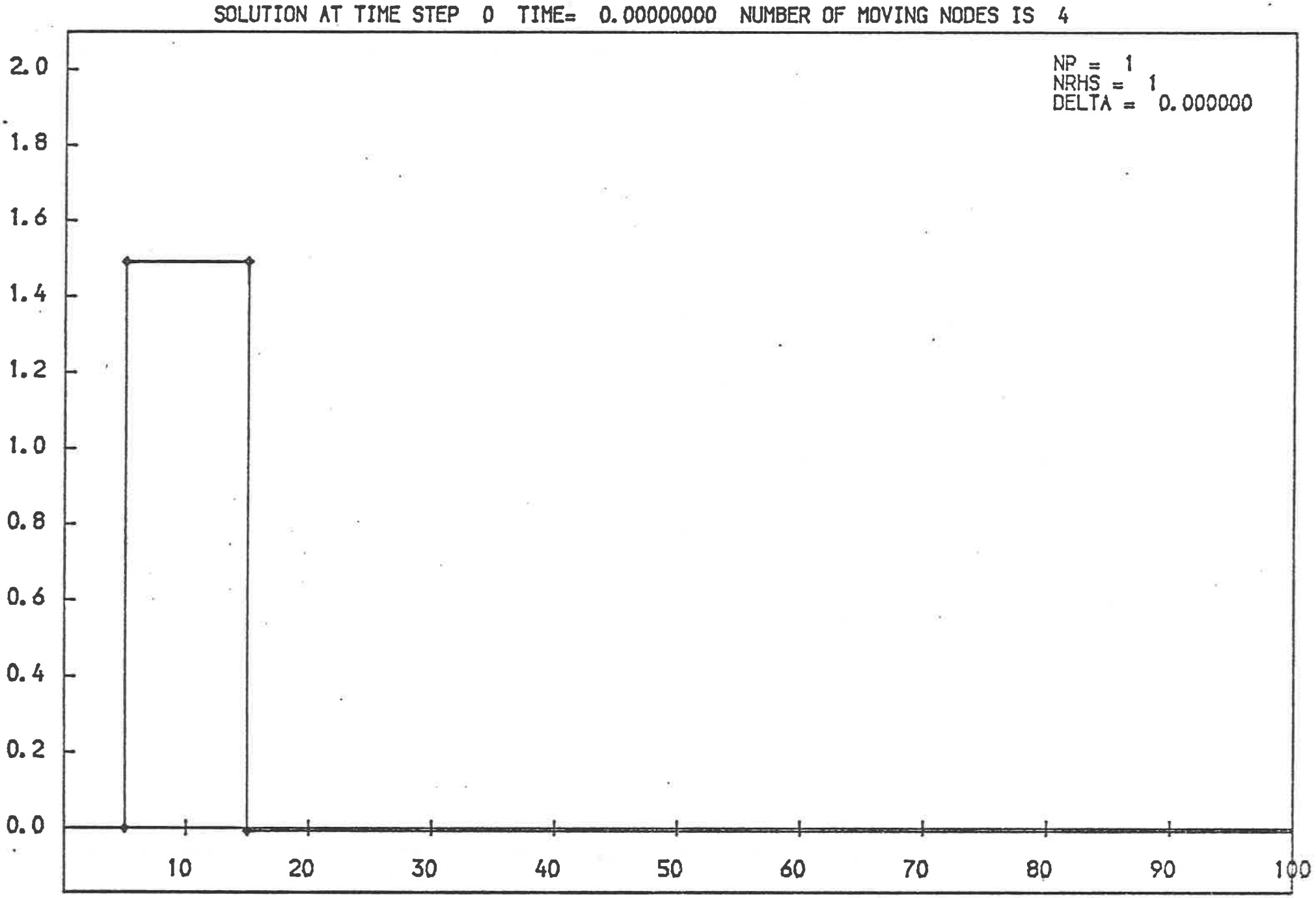
SOLUTION AT TIME STEP 0 TIME= 0.00000000 NUMBER OF MOVING NODES IS 4
NP = 1
NRHS = 1
DELTA = 0.000000
2.0
1.8
1.6
1.4
1.2
1.0
0.8
0.6
0.4
0.2
0.0
10
20
30
40
50
60
70
80
90
100

FIG. 4.1

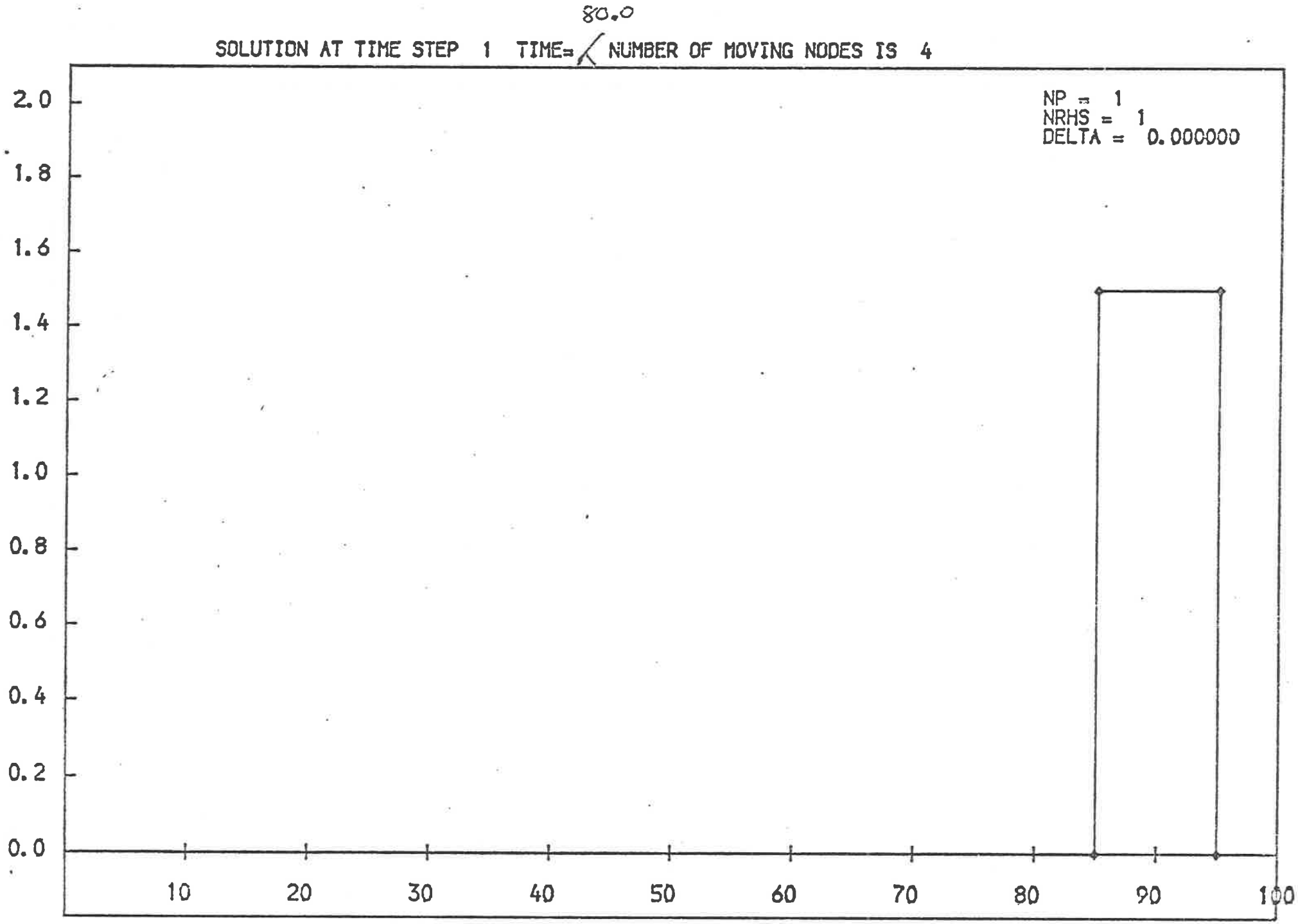
80.0
SOLUTION AT TIME STEP 1 TIME=
NUMBER OF MOVING NODES IS 4
NP = 1
NRHS = 1
DELTA = 0.000000
2.0
1.8
1.6
1.4
1.2
1.0
0.8
0.6
0.4
0.2
0.0
10
20
30
40
50
60
70
80
90
100

FIG. 4.2

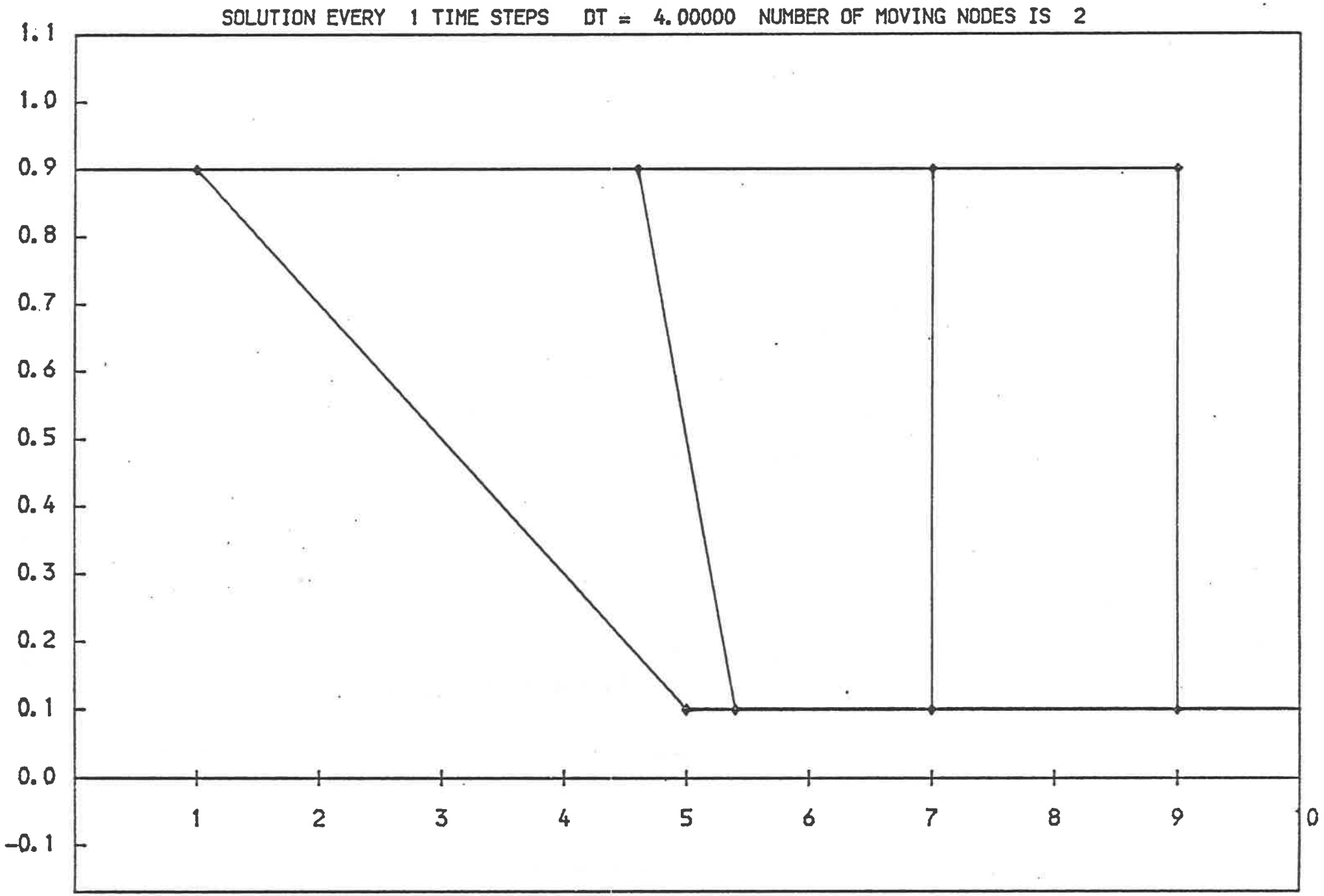
SOLUTION EVERY 1 TIME STEPS DT = 4.00000 NUMBER OF MOVING NODES IS 2
1.1
1.0
0.9
0.8
0.7
0.6
0.5
0.4
0.3
0.2
0.1
0.0
-0.1
1
2
3
4
5
6
7
8
9
0

FIG. 4.3

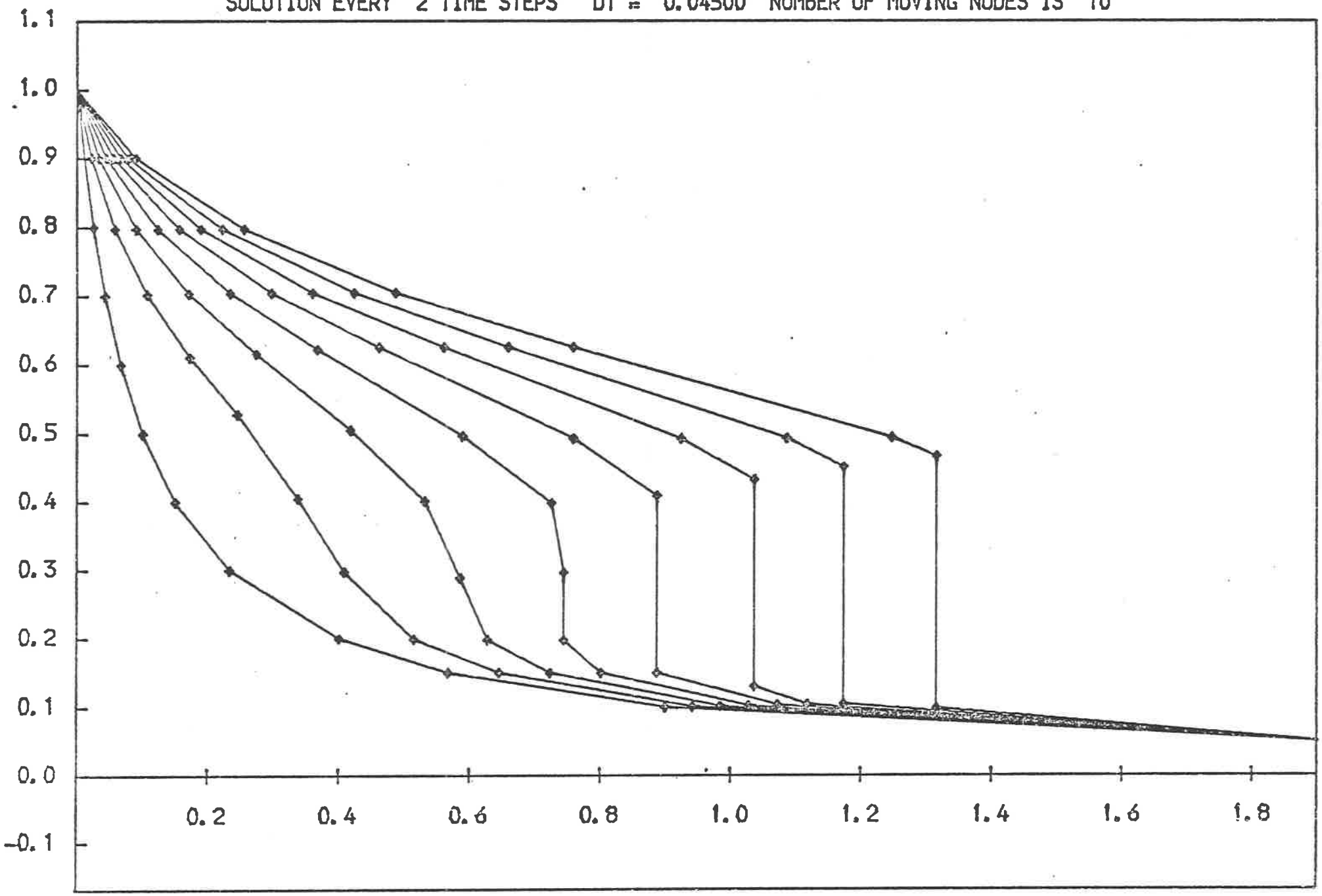
SOLUTION EVERY 2 TIME STEPS DT = 0.04500 NUMBER OF MOVING NODES IS 10
1.1
1.0
0.9
0.8
0.7
0.6
0.5
0.4
0.3
0.2
0.1
0.0
-0.1
0.2
0.4
0.6
0.8
1.0
1.2
1.4
1.6
1.8

FIG. 4.4

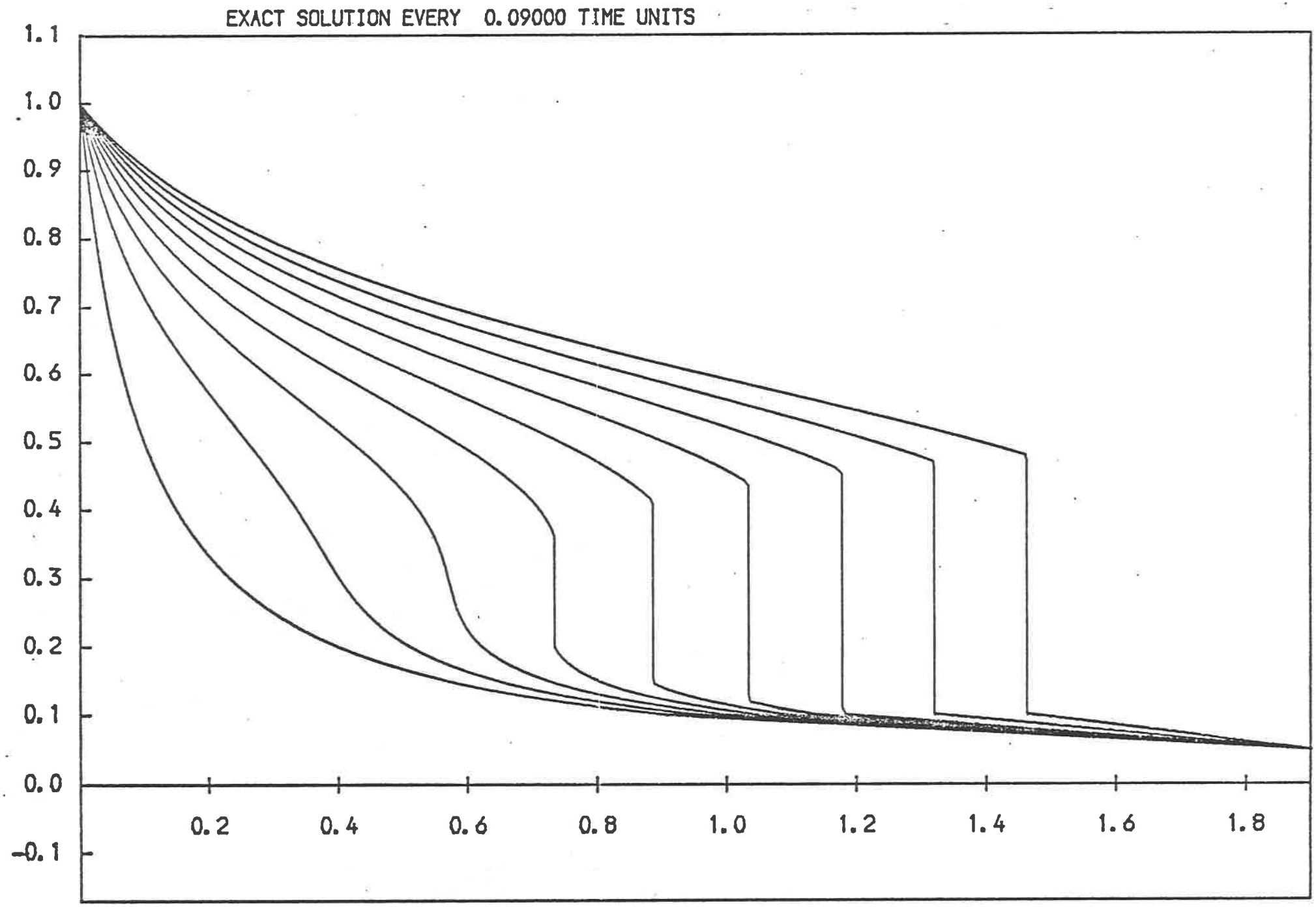
EXACT SOLUTION EVERY 0.09000 TIME UNITS
1.1
1.0
0.9
0.8
0.7
0.6
0.5
0.4
0.3
0.2
0.1
0.0
-0.1
0.2
0.4
0.6
0.8
1.0
1.2
1.4
1.6
1.8

FIG. 4.5

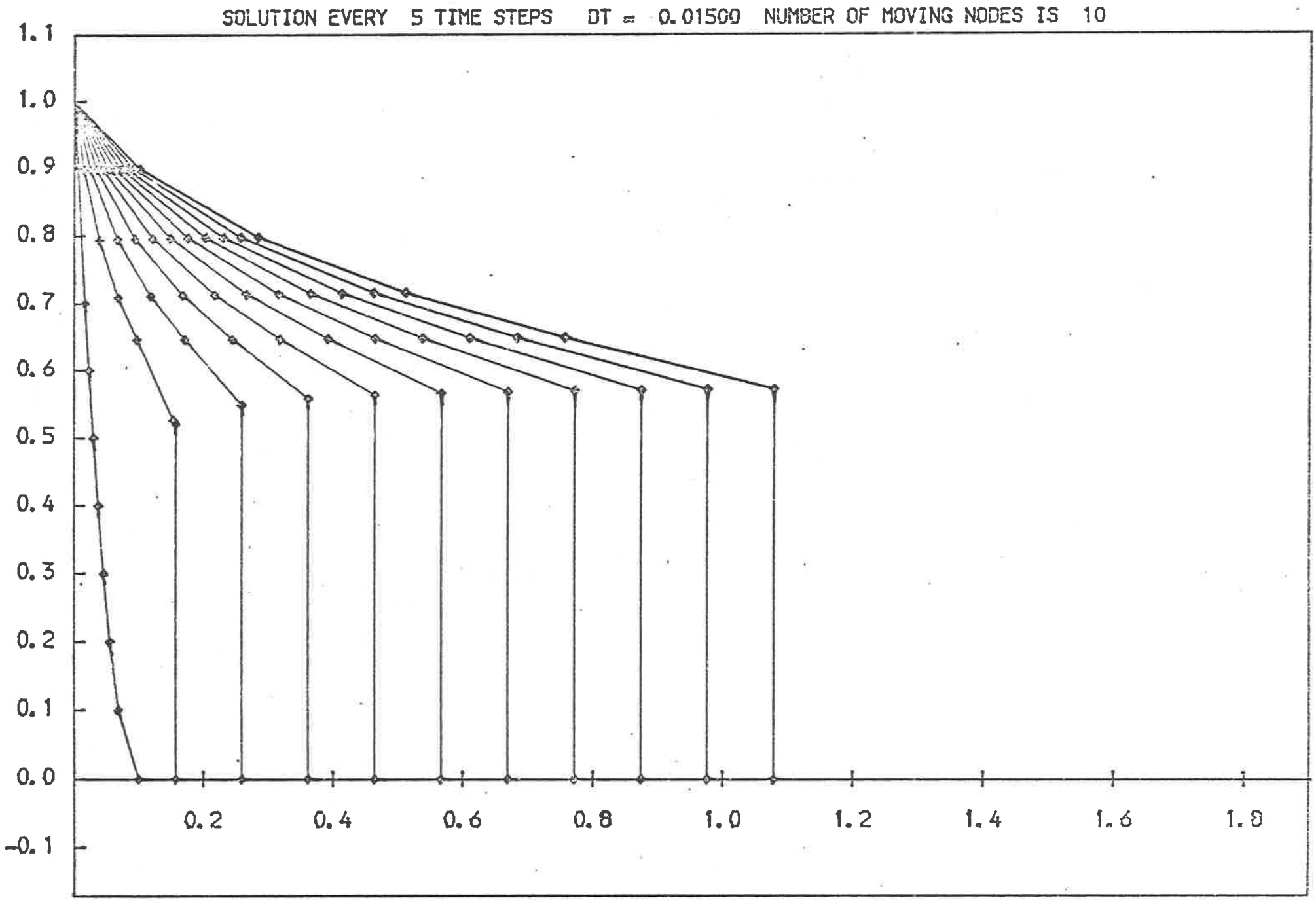
SOLUTION EVERY 5 TIME STEPS DT = 0.01500 NUMBER OF MOVING NODES IS 10
1.1
1.0
0.9
0.8
0.7
0.6
0.5
0.4
0.3
0.2
0.1
0.0
-0.1
0.2
0.4
0.6
0.8
1.0
1.2
1.4
1.6
1.8

FIG. 4.6

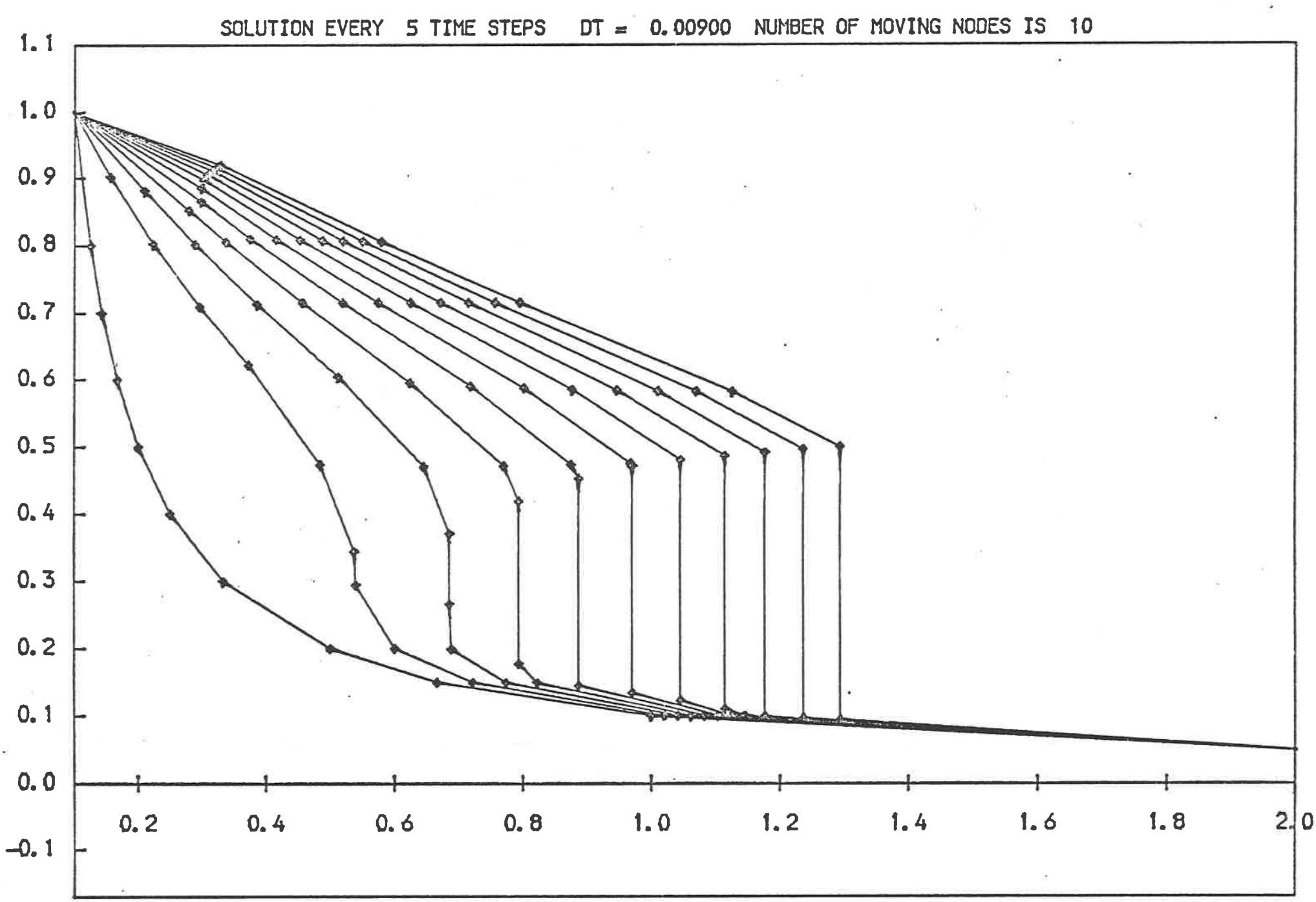
SOLUTION EVERY 5 TIME STEPS DT = 0.00900 NUMBER OF MOVING NODES IS 10
1.1
1.0
0.9
0.8
0.7
0.6
0.5
0.4
0.3
0.2
0.1
0.0
-0.1
0.2
0.4
0.6
0.8
1.0
1.2
1.4
1.6
1.8
2.0

FIG. 4.7

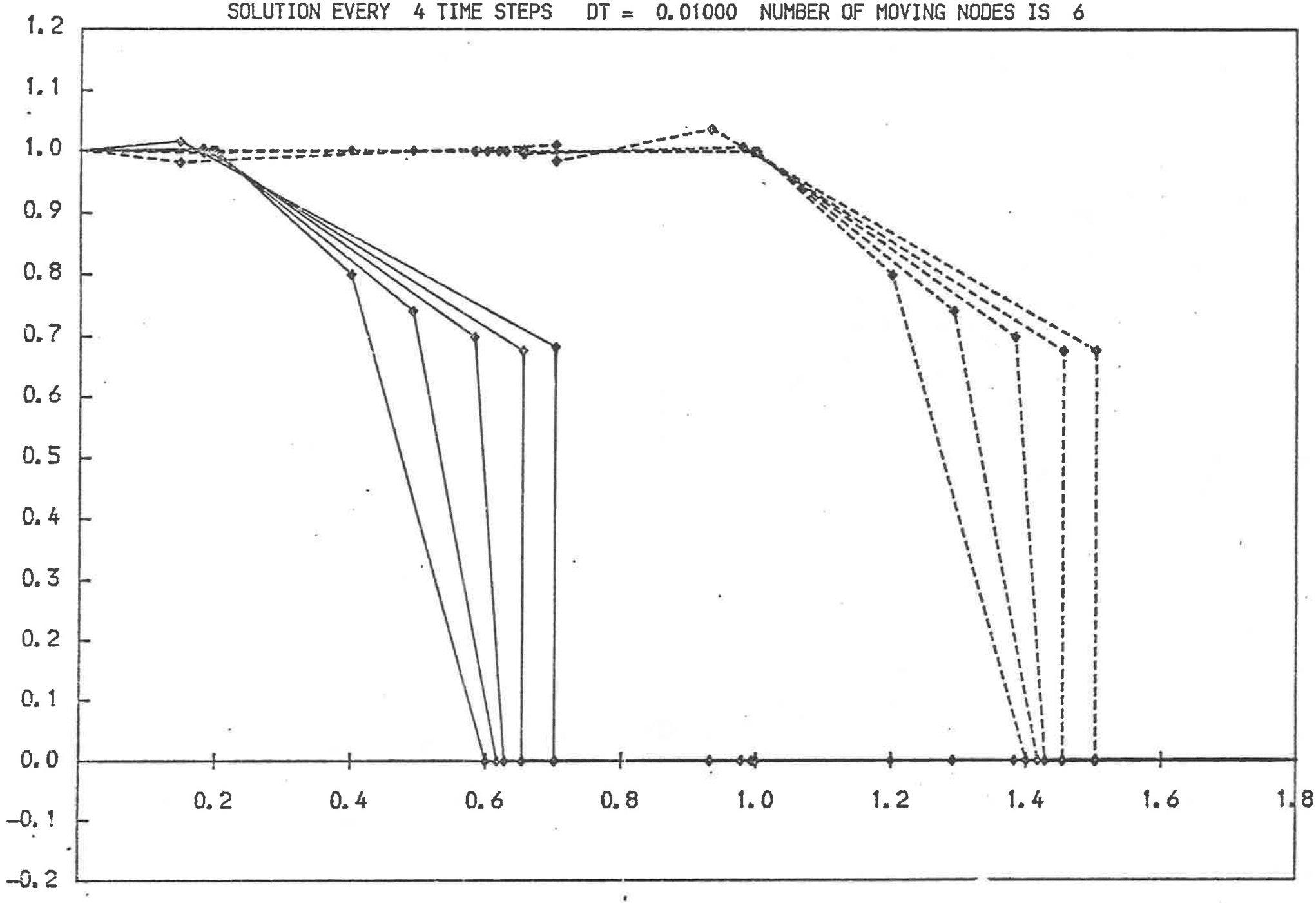
SOLUTION EVERY 4 TIME STEPS DT = 0.01000 NUMBER OF MOVING NODES IS 6
1.2
1.1
1.0
0.9
0.8
0.7
0.6
0.5
0.4
0.3
0.2
0.1
0.0
-0.1
-0.2
0.2
0.4
0.6
0.8
1.0
1.2
1.4
1.6
1.8

FIG. 4.8

The problem of parallelism has been studied and a simple and effective remedy proposed.

By directly applying the Rankine-Hugoniot conditions - which is accomplished naturally and easily with this moving mesh method - excellent modelling of pure shocks has been obtained.

Considerably more work needs to be done on application of the method to systems of equations. Indeed it appears that there has been very little mathematical analysis of the actual systems of equations describing three-phase flow. A very useful 'test-bed' system (which arises in aerodynamics) is presented by Roe in [12], and hopefully something equivalent arising in the problems of oil recovery will soon be proposed.

Finally extension of the method to two dimensional problems must be regarded as the very important next step.

Acknowledgements

It is with pleasure that I acknowledge the help and encouragement given to me by Professor K.W. Morton and Dr. M.J. Baines throughout this work, and the invaluable help given by Dr. Baines in writing this report.

I also wish to thank British Gas, London Research Station for their support and interest over the last year.

References

[1] P. Concus & W. Proskurowski. Numerical solution of a non-linear hyperbolic equation by the Random Choice Method. J. Comp. Phys. 30, 1979, 153-166.

[2] G. Chavent. About the identification and modelling of miscible or immiscible displacements in Porous Media. Lecture notes in Control and Information Sciences Vol. 1, Springer-Verlag (1976).

[3] J. Douglas, Jr. Simulation of miscible displacement in porous media by a modified method of characteristic procedure. Proc. 9th Biennial Conf. on Numerical Analysis, University of Dundee, 23-26 June, 1981.

[4] J. Glimm, D. Marchesin & O. McBryan. A numerical method to two phase flow with an unstable interface. J. Comp. Phys., 39, 1981, 179-200.

[5] L. Dake. Fundamentals of Reservoir Engineering. Elsevier: Developments in Petroleum Science 8 (1978).

[6] K. Aziz & A. Settari. Petroleum Reservoir Simulation. Applied Science Publishers: London (1979).

[7] S. Buckley & M. Leverett. Mechanism of fluid displacements in sands. Trans. AIME 146 (1942), 107-116.

[8] I. Cheshire, J. Appleyard, D. Banks, R. Crozier & J. Holmes. An efficient fully implicit simulator. Paper presented at the European Offshore Petroleum Conference and Exhibition, London October 21-24 1980.

[9] D. Peaceman. Fundamentals of Numerical Reservoir Simulation. Elsevier: Developments in Petroleum Science 6 (1977).

[10] J. Rae. Variational methods in oil reservoir modelling. Proc. Sparse Matrix Conf., Reading University, June 1980.

[11] B. Engquist & S. Osher. One-sided difference approximations for non-linear conservation laws. Math. Comp. 36 No. 145, 321-352 (1981).

[12] P. Roe. Numerical modelling of shockwaves and other discontinuities. Paper presented at IMA Conf. on Numerical Methods in Computational Aerodynamics, University of Reading, 29th March - 1st April 1981.

[13] K. Miller & R. Miller. Moving Finite Elements, Part I. SIAM J.N.A. 18, No. 6, 1019-1032 (1981).

[14] K. Miller. Moving Finite Elements, Part II. SIAM J.N.A. 18, No. 6, 1033-1057 (1981).

[15] B. Herbst, A. Mitchell & S. Schoombie. A moving Petrov-Galerkin Method for Transport Equations (1981).

[16] R. Gelinas, S. Doss & K. Miller. The Moving Finite Element Method: Applications to General Partial Differential Equations with Multiple Large Gradients. J. Comp. Phys. 40, (1981), 202-249.

[17] M.J.P. Cullen & K.W. Morton. Analysis of Evolutionary Error in Finite Element and other methods. J. Comp. Phys. 34 (1980), 245-267.

[18] K. Johnson, R. Lewis & K. Morgan. An Analysis of Oscillations in the Finite Element Modelling of Buckley-Leverett Problems. Proc. BAIL I Conf. Trinity College, Dublin, 3-6 June, 1980.

[19] I. White, R. Lewis & W.L. Wood. The numerical simulation of multiphase flow through a porous medium and its application to reservoir engineering. App. Math. Modelling 5 (1981) 165-172.

[20] R.J. Leveque. Large time-step shock capturing techniques for scalar conservation laws. Dept. of Computer Science, Stanford University (1982).